Malaysian Journal of Computer Science, Vol. 18 No. 1, June 2005, pp. 1-19

A MULTIPARAMETER HIERARCHICAL REPRESENTATION USING REGION-BASED ESTIMATION MODEL FOR DETECTING TUMOR IN T2-WEIGHTED MRI BRAIN IMAGES

Phooi Yee Lau and Shinji Ozawa
Graduate School of Science and Technology
Keio University
3-14-1 Hiyoshi, Kohoku-ku, 223-8522 Yokohama
Japan

ABSTRACT

The objective of this paper is to present an analysis method for digitised medical images to allow diagnosis and interpretation for medical practitioners or medical students. A simple diagnosis method was developed using multiparameter value; edge (E), gray (G), and contrast (H), to develop a decision support system for interpreting and analysing T2-weighted MRI brain images. The hierarchical representation proposed here is able to study the sub-regions EGH parameter in comparison with the estimation model for abnormal occurrences, and depending on the regions of abnormality, diagnosis and prescription is provided. In this paper, three different experiment sets are introduced to study the proposed method: 1) Set I: different time interval images, 2) Set II: different brain disease images, and 3) Set III: multiple slice images from different age and gender. Experimental results illustrates that our proposed technique here incurred an overall error smaller in comparison with our previous proposed method. In particular, the proposed method allowed decrements of false alarm and missed alarm, which demonstrates the effectiveness of our proposed technique. In this paper, we also present a prototype system, known as PCB, to evaluate the performance, accuracy and robustness of the algorithms and reveal the proposed approach capabilities in interpretation and diagnosis.

Keywords: ***Image classification, Medical imaging, Multiparameter, Estimation model, Hierarchical representation, Brain tumor***

1.0 INTRODUCTION

Today, technological advances have far outgrown our envisioned directions a decade ago. We have never anticipated that medical imaging would make such a vast impact on science, engineering and medicine. In the medical imaging field, the on-going research for a better front-end technology, incorporating medical-like capabilities to produce an intelligent system such as the application of cognitive science in computer-assisted medical diagnosis is certainly the success of what we hope to see in the near future. Over the past few years, we have seen an increasing amount of research in areas of image processing, but it has not yet been broadly applied as a computer-assisted diagnostic tool in a clinical environment. We believe diagnostic research-oriented system having the capability to classify healthy and cancer patients shall become the next pressing issue. We are moving towards a proactive diagnostic system, whereby computers may anticipate and provide treatment programs, and the study and experimentation in this discipline in terms of diagnosis accuracy and risk assessment are necessary because patients are now looking at healthcare services from a higher perspective.

This paper first studies the important visual attributes of a normal aging T2-weighted MRI brain images, and categorised the important attributes found into three parameters; edge, gray, and contrast. Then using hierarchical knowledge representation, we effectively associate the object with pixels and regions to describe the features present in an image. The selection of the features is important because they determine the diagnostic accuracy and robustness. Using features identified in a normal healthy brain, we first ensemble these brain images to develop the estimation model which are able to classify input images (problem case) for diagnosis and interpretation. We implemented our proposed approach on three different experimental datasets:

1) Set I: Periodical image;
2) Set II: Different neoplastic and infectious diseases, and;
3) Set III: Different age and gender.

2.0 RELATED WORK

In our earlier paper, we proposed a universal classification method to support the classification of medical images from different imaging modalities for the classification block [1, 2]. Later, we proposed using multiple classifier for image registration applied in multimodal images for the registration block [3]. Also, studies on the methodology in segmentation, classification, analysis, registration, search and sort to obtain an economic model has been discussed and explored [4]. Fig. 1 shows the conceptual framework of the image-guided medical diagnostic system, focusing on major fundamental image processing components, which is sufficiently robust and can be applied in a clinical environment.

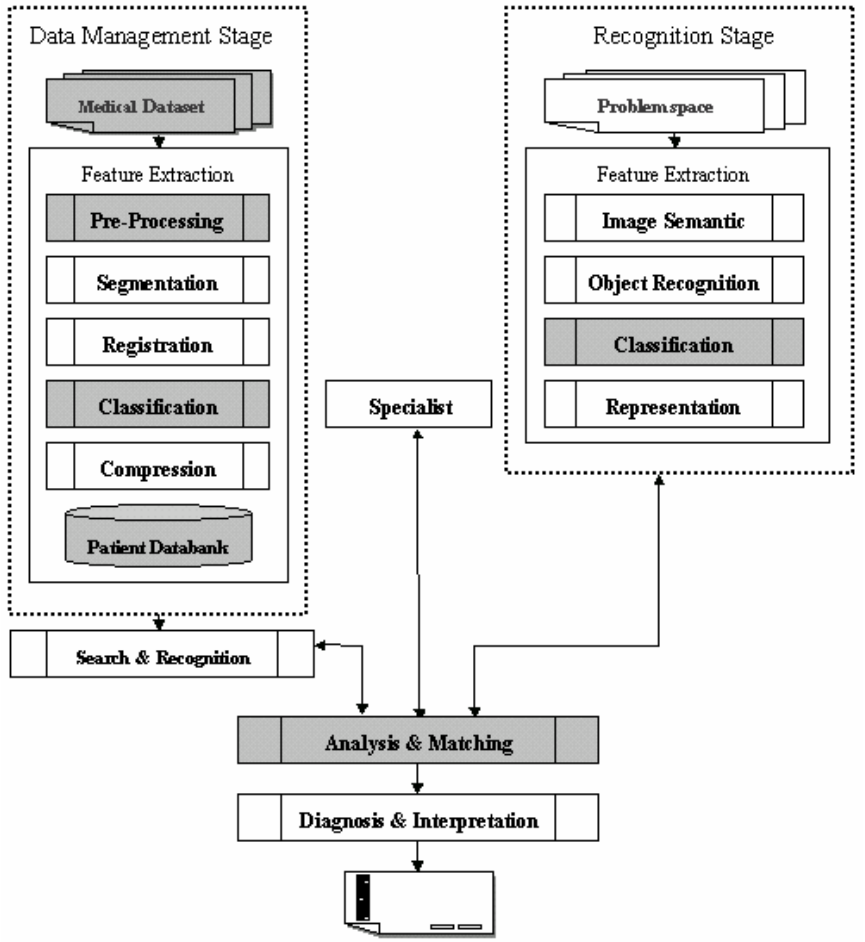

Fig. 1: Framework for the image-guided medical diagnostic model

3.0 METHODOLOGY

Fig. 2 shows the block diagram of our proposed approach structure. Our proposed approach in this research includes the pre-processing block, employed to identify and preview input images or the subject according to age, gender and imaging modality. This paper first studies the important visual attributes of normal aging brain images, and categorizes important parameters found, e.g. in terms of texture, content, and shape. Further studies reveal that we can represent these important parameters using image-processing techniques. Here, we represent these features on images by: (1) the edge (E) for shape feature, (2) grayscale (G) for texture features, and (3) contrast (H) for content features. We combine these features to develop a multiparameter value for representing the whole brain, and to develop an estimation model using healthy brain dataset. Finally, we study the hierarchical representation of the brain to obtain the exact location of the tumor for diagnosis and interpretation and gain new insights into cancer detection and treatment.

In defining a region, we analyse input images whereby we observed that brain regions are highly dependable on its image region of interest (*ROI*) and not its actual image size, or the structure of interest (*SOI*). The image *ROI* is divided into regions (*r, c*) identified using the edges (*E*) parameter, gray values (*G*) parameter, and local contrast (*H*) parameter. These multiparameter values of each region will be classified as either malignant (tumorous) or normal.

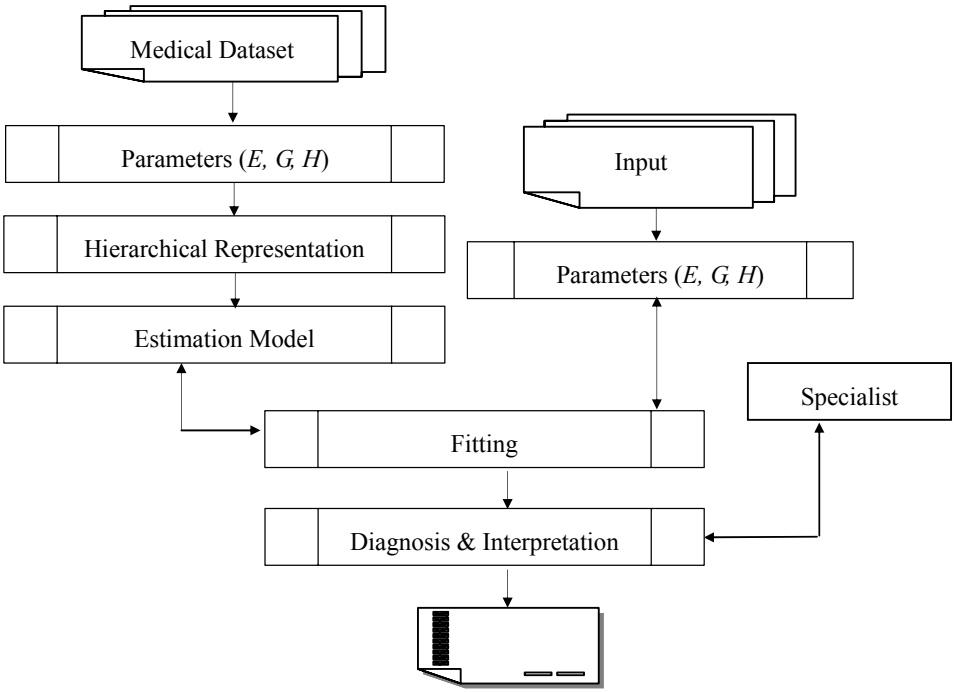

Fig. 2: Proposed structure for image recognition process

In this paper, we focused on analysing T2-weighted MRI images because medical practitioners often can diagnose whether a brain tumor exist within a T2-weighted MRI images with sensitivity of 94% [5]. Other imaging modalities like PET or PET/CT, apart from being an expensive diagnostic imaging tool, have the capability to diagnose primary tumors accurately in any part of the body. The patient is only injected with an extremely low dose of radioactive sugar-based tracing agents into the bloodstream. When radiation is emitted from cells that are very metabolically active, such as malignant tumor cells, the PET scanner detects them. Due to the higher cost of PET scans, for patients with signs or symptoms suggestive of tumors, a variety of noninvasive tests, including CT, MRI, US (Ultra Sound) or X-ray may be undertaken prior to the PET scan. T2 weighted MRI is reported to be highly sensitive for detecting brain abnormalities in Multiple Sclerosis (MS) and other Systemic Immune mediated Diseases (SIDs) and CNS lesions in patients [6, 7].

3.1 Pre-Processing

The pre-processing block consists of image previewing function and image adaptation function, as shown in Fig. 3. PCB v.2 system only accepts bitmapped images. The image adaptation function is needed to prepare the input images for their subsequent processing, due to the reasons listed below:

1) Raw images obtained from the Visible Human (labeled male) are compressed using the Joint Photographic Experts Group (JPEG) compression scheme using a quality factor of 75
2) The Whole Brain Atlas v. 1.0 is primarily organised and stored as Graphic Interchange Format (GIF) files.

3.2 Classification

Post-processing images will be further processed in the image classification block, and evaluated using the proposed techniques. In the selection of a suitable approach, we have studied some previous methodologies developed [8, 9, 10, 11]. Vailaya (2001) analyses low-level image features in classifying input images as an indoor or outdoor image using hierarchical classification method. Abassi (2001) studied the image contour to develop a shape-based retrieval system. Epifiano (2002) proposed global framework for texture classification based on pixel-based random closed set theory. From these literatures, we are able to conclude that the analysis structure within medical images is an important feature in any image for all applications. In this paper, we divide the section into three sub-sections; the multiparameter features, the hierarchical representation, and the estimation model.

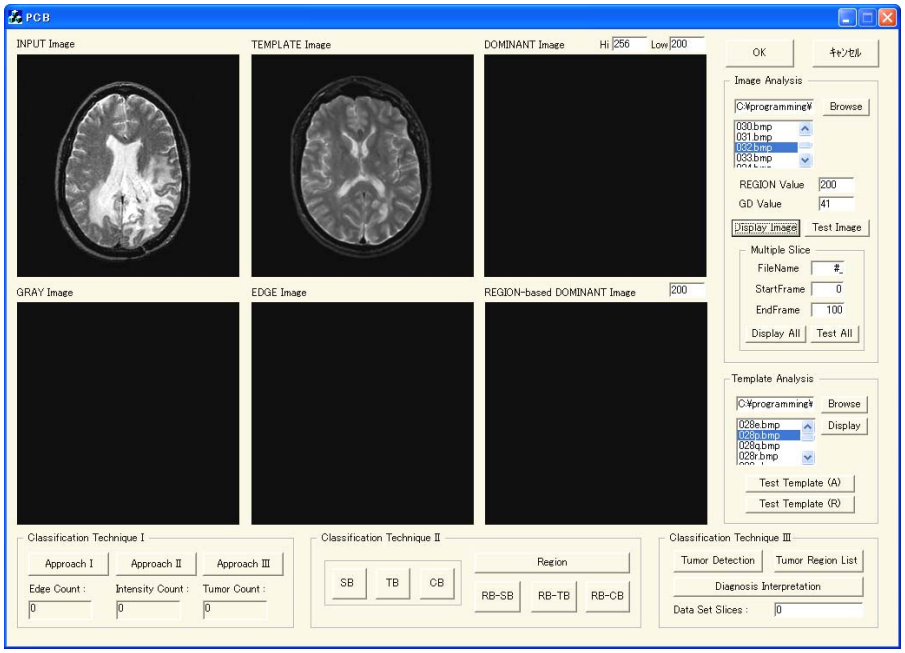

Fig. 3: Image Previewing in the Pre-Processing Block

3.2.1 Multiparameter Features

Recent advances in medical image analysis often require an image to be segmented into several parameters, to address the different aspects of analysing the image into anatomically and pathologically meaningful regions. Classifying regions using multiparameter values makes the study of the regions of physiological and pathological interest easier and more definable. Here, multiparameter features refer to the following three specific features: the edges (E), gray values (G), and local contrast (H) of the pixels.

In most medical images, the structure of interest (tumors, lesions arterial structures, etc.) occupies a percentage of the pixels that is often much below 10% of all pixels [12]. Therefore, for analysis of such small tissues or structures, we proposed a block system that divides the structure of interest (*SOI*) which is highly dependant on imaging modalities, into region size (W) and image size (*ROI*). Region (R) is denoted as a part of the whole image (*ROI*), shown in Fig. 4. The *ROI* is divided evenly by a factor of eight; else, the dimensions are padded out with the average pixel value (P_{AVE}) to give dimensions that are a factor of 8.

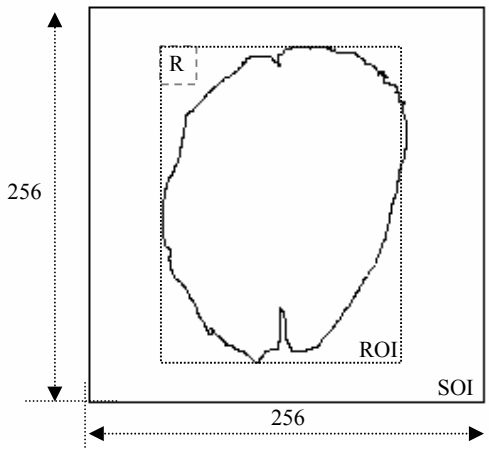

Fig. 4: *ROI* of an input image (128 x 128) with region size *R* (8 x 8 pixel)

3.2.1.1 Edge Parameter

Edge information is often used to determine boundaries of object, which are mainly used for analysis to derive the similarity criterion of a pre-determined object. In our earlier findings, we observe that the edge attribute for a tumor image and non-tumor image is different, visually and quantitatively, as shown in Fig. 5. The reduction of edge count for tumor images is because the brain substance is pushed aside and compressed by the presence of a brain tumor, symptoms occur due to the local effects of cerebral tissue compression or invasion. Dr. A. Vincent Thamburaj, a neurosurgeon from Apollo Hospitals in Chennai (India) reports that systemic malignancy can metastasize to any location in the brain but most commonly (80%) affects the cerebral hemispheres, which accounts for the tendency of metastases to be located at the gray-white junction [13]. White matter lesions appear as high intensity regions in both proton density weighted and T2-weighted MRI images of the brain and the cerebral compression incidences reduce the edge count of the cerebral hemisphere, in comparison with normal healthy brain images [14]. Our findings conclude that the edge count of the normal brain contain a reasonable amount of edges because the gray matter (*GM*) of the brain is evenly distributed. Utilising this understanding, we use the Sobel edge detection method to detect image edges (I_E). Compared to our previous proposed algorithm, we propose a slightly different threshold value to be used [15]. In many cases, finding one threshold compatible to the entire image is very difficult. In view of this, our paper proposes the adaptive image binarization (I_B) where the threshold value is named as the global discriminate value (G_D). This value is calculated using the average pixel value (Iav_s) of each image slice (S) for total image slices (T) of an image dataset, shown in Equation (1) and Equation (2).

$$Iav_s = \frac{1}{65536}\sum I_s(x, y) \tag{1}$$

$$G_D = \frac{\sum_{s=0}^{T} Iav_s}{\mathrm{T}} \tag{2}$$

Given two images, I_E and I_B, the edge parameter (E) is increased by one each time when $I_E\,(x, y) =$ '1' and $I_B\,(x, y) =$ '1' meet, or when both images processed using different processing method have a value of '1' at the same point, shown in Equation (3).

$$E_{(r,\ c)} = \sum_{(x,y)\in R} (I_{Ep} == 1 \,\&\, I_{Bp} == 1) \tag{3}$$

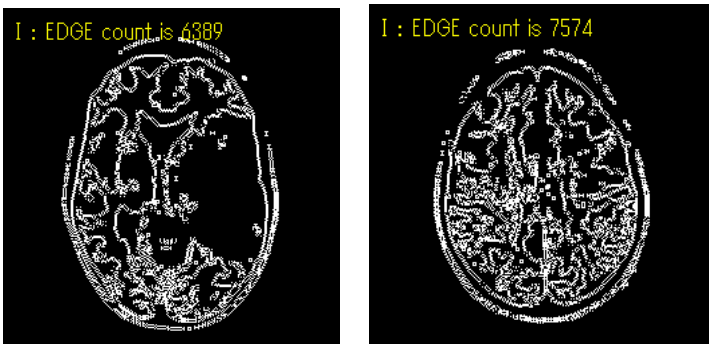

(a) (b)

Fig. 5: Brain image (a) is taken from Case 28, where tumor is found and the edge count is minimum, compare with non-tumor gray matter in brain image (b)

3.2.1.2 Gray Parameter

In this technique, the gray parameter (G) of the brain of each region is accumulated, controlled using a binary image using the G_D value as a threshold value, as shown in equation (4). Here, we assumed that pixel value below the G_D value consist mostly of noises and image reconstruction weakness. Krishnan (1998) describes how each pixel from an MR image represents many tissue parameters, typically, proton density (PD), spin-lattice (T1) and spin-spin (T2) relaxation time [16]. Thamburaj also specifies that malignant tumor cells contain highly proteinaceous fluid and is represented by high signal intensity on T2-weighted MRI images of the brain [13]. It is reported that textural features contain information about the spatial distribution of tonal variations [17]. The concept of tone is based on the intensity of pixels within a defined region (shades of gray in a grayscale image). All these studies assume that textural features can be used to classify the T2-weighted MRI images using the spatial pixel intensity values in association with the brain tissue. Here, using the VHD (male) dataset, we calculate the pixel representation on T2-weighted MRI brain images, whereby the pixel ratio of the image is 1.016 mm/pixel (256 x 256 pixels within the actual head dimensions of 260.0mm x 260.0mm), for further understanding. Here, the pixels intensities are computed for studying both the healthy and cancer patients, using Equation (4).

$$G_{(r,c)} = \sum_{(x,y)\in R} I_P(x,y) \quad \text{, if } I_B(x,y) = 1 \tag{4}$$

3.2.1.3 Contrast Parameter

Contrast (H) is often used to characterize the extent of variation in pixel intensity. In this technique, we study the difference, especially a strong dissimilarity, between entities or objects in an image $I(x,y)$ using an adaptive region-based linear contrast enhancement algorithm. We adopt the minimum/maximum stretch algorithm in the 8-neighborhood connectivity, where S_{min} and S_{max} is the minimum and maximum intensity value of the neighborhood, shown in Equation (5). By studying the relational features of an image, high contrast parameter value among pixels can be filtered and calculated. In our previous studies, tumor cells are often associated with higher value of contrast parameter (H). H_d is obtained by totaling the contrast of a region, shown in Equation (6).

$$I_H(x,y) = \left(\frac{I(x,y) - S_{\min}}{S_{\max} - S_{\min}} \right) \times S_{\max} \tag{5}$$

$$H_{d(r,c)} = \sum_{(x,y)\in R} I_H(x,y) \tag{6}$$

3.2.2 Hierarchical Representation

Features representing individual pixels or regions (group of pixels) in an image play a critical role in image analysis. We study the hierarchical representation or framework of an object because it is important to obtain a general structure of an image or a scenario, which can often be divided into a set of small scenes or knowledge domains in the corresponding images to perform a computerised analysis. We apply low level analysis incorporating a bottom-up approach for multiparameter features in a region-based model, as shown in Fig. 6.

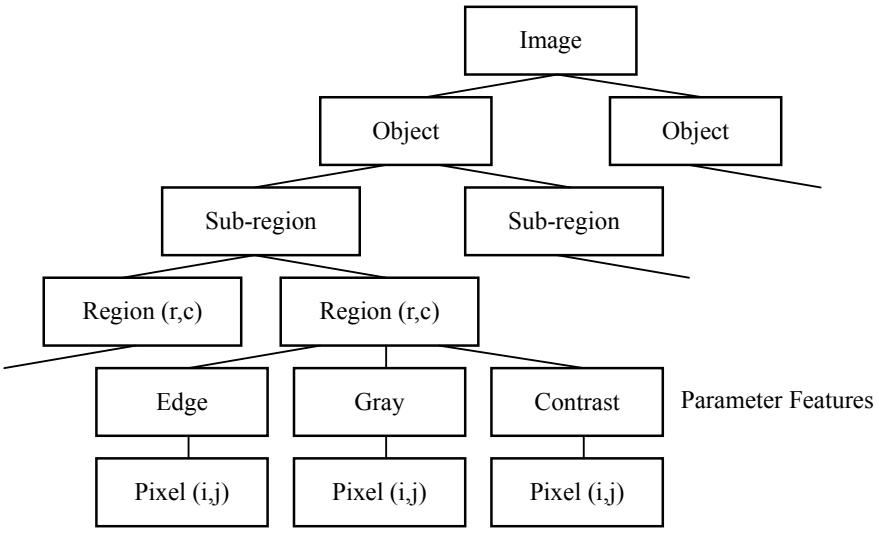

Fig. 6: Region-based hierarchical representation (low-level analysis)

The sub-region is segmented based on the features of the images. Fig. 7 shows the feature point of the object in the template, which is then used to distinct and segment the images into sub-regions. The correlation and structural arrangement of the whole brain is similar on both side. In a normal brain, studying the elements occurrence on one half of the brain should incur the same results for the other half. In abnormal occurrence in regions, and depending on the regions of the abnormality, diagnosis and prescription will be provided using the estimation model. (Note: Several MRI-based studies of age-related volumetric changes in the gray and white matter of healthy volunteers have been reported [18]).

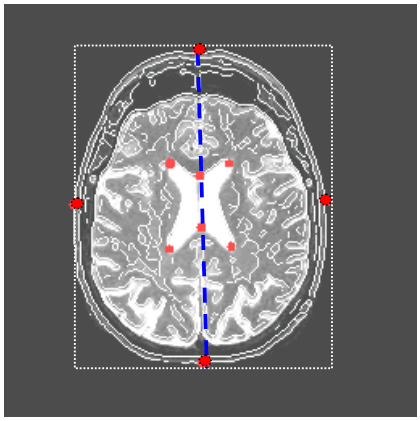

Fig. 7: The feature points of the template for sub-region segmentation for fitting purposes

3.2.3 Estimation Model

An estimation model requires all parameters obtained using priority knowledge on a set of images, obtained from normal aging brain images. This knowledge is ensembled using the hierarchical representation technique in an 8 by 8 pixel region of the *ROI* in the T2-weighted MRI brain images. Due to the relatively small number of training set (from normal aging T2-weighted MRI brain images), averaging over a small neighborhood of regions around the *ROI* is performed. The estimation model is divided into image slice and position, *I(i,j,k)*, as shown in Fig. 8.

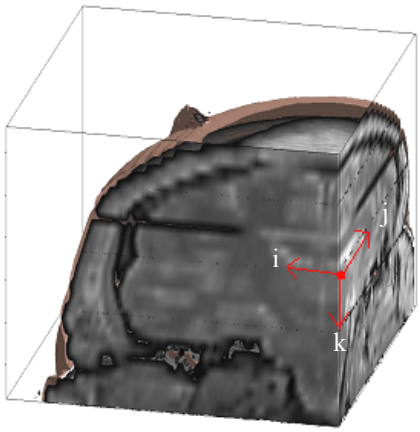

Fig. 8: The estimation model from a normal aging brain image

4.0 MATERIALS

4.1 Hardware and Software Environment

The experiment is implemented using MATLAB and Visual C++ on a Dell Dimension 8400 Pentium IV 3.20GHz computer with 1 GB RAM. MATLAB is the support analysis software used in this paper. The core software, PCB, has been developed in the Ozawa Laboratory at Keio University using Visual C++ programming language on bitmapped medical images (**http://www.ozawa.ics.keio.ac.jp**). PCB is a diagnostic research-oriented system with the capability to detect tumor images on bitmapped medical images, and to make correlations between a disease and its properties with its clinical management. Another supporting software is the Visible Human 2.0 system.

4.2 Image Material

In order to evaluate the performance of our proposed algorithms and methodology, the experiments were conducted on two data sets.

1. The Visible Human (male) CD provided by Research Systems (http://www.rsinc.com).
2. The Whole Brain Atlas v. 1.0 (Case 1, Case 5, Case 9, Case 26, Case 28, Case 32, Case 33, and Case 36) provided by the Departments of Radiology and Neurology at Brigham and Women's Hospital, Harvard Medical School, The Library of Medicine and the American Academy of Neurology (http://www.med.harvard.edu/AANLIB/home.html).

5.0 IMPLEMENTATION RESULTS

In this section, we present three sets of experiments, namely, Set I, Set II, and Set III. Set I constitutes two-dimensional images with infectious brain disease obtained from the same patient over a long period of time. Set II contains five different neoplastic and inflammatory brain diseases images: Metastatic Adenocarcinoma, Glioma, Metastatic Bronchogenic Carcinoma and Multiple Sclerosis. A malignant neoplastic disease is a malignant growth or tumor caused by an abnormal and uncontrolled cell division. It may spread to other parts of the body through the

lymphatic system or the blood stream. An inflammatory brain disease is characterised by inflammation, a response of body tissues to an injury or irritation. Set III consists of multiple slices of T2-weighted MRI brain images from different disease, age, and gender from both healthy and cancer patients. The three different experiment dataset is used to compare the performance and robustness of the method proposed. Experimental results demonstrated the robustness of the proposed image classification system in detecting brain tumor in T2-weighted MRI brain images.

5.1 Set I: Different Time Lapse Images

The proposed technique is tested on a series of T2-weighted MRI brain images from Case 5. The image is taken from a patient with a chronic progressive form of disease in twenty-three different intervals showing multiple sclerosis lesion evolution over a period of one year. Fig. 9 shows an image slice of the experiment set that has undergone image registration with a region-based image using the mutual information technique proposed in our earlier paper [3]. This image is used to further study and extract the region of interest and infectious area from the whole image.

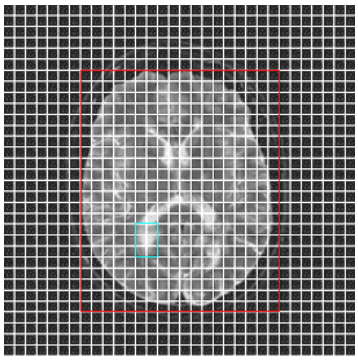

Fig. 9: Regionalise image using 8 x 8 pixel window: Row 21 to Row 23 of Column 13 to Column 14 is detected of having multiple sclerosis

In order to demonstrate the robustness property of multiparameter techniques, a series of experiments on this image dataset has been proposed. The *E* parameter, *G* parameter and *H* parameter is analysed on slice 19 (r interval), 20 (s interval), 21 (t interval), 22 (u interval), and 23 (w interval) of this experimental set. Experimental results shown in Fig. 10 reveal the parameter differences on normal aging images (plus [+] and square [□] point) and infectious diseases images (diamond [◊] point). The diamond points are found relatively far from the plus points and square points suggesting an abnormality in these regions on the images. Further experimental results shown in Fig. 11 have revealed a strong representation of the reoccurrence of the lesion over different time frames at a specific region, for studying the strong representation of infectious area (bold line [diamond]) vs. normal properties (dotted line [plus] and dashed line [square]) of the T2-weighted MRI brain image, compared with the previous approach [2]. In experimenting Set I, we have shown that our proposed method is able to detect and discerned the minuscule differences between two images. Fig. 12 shows the PCB system result, marking all suspected blocks that have minuscule changes.

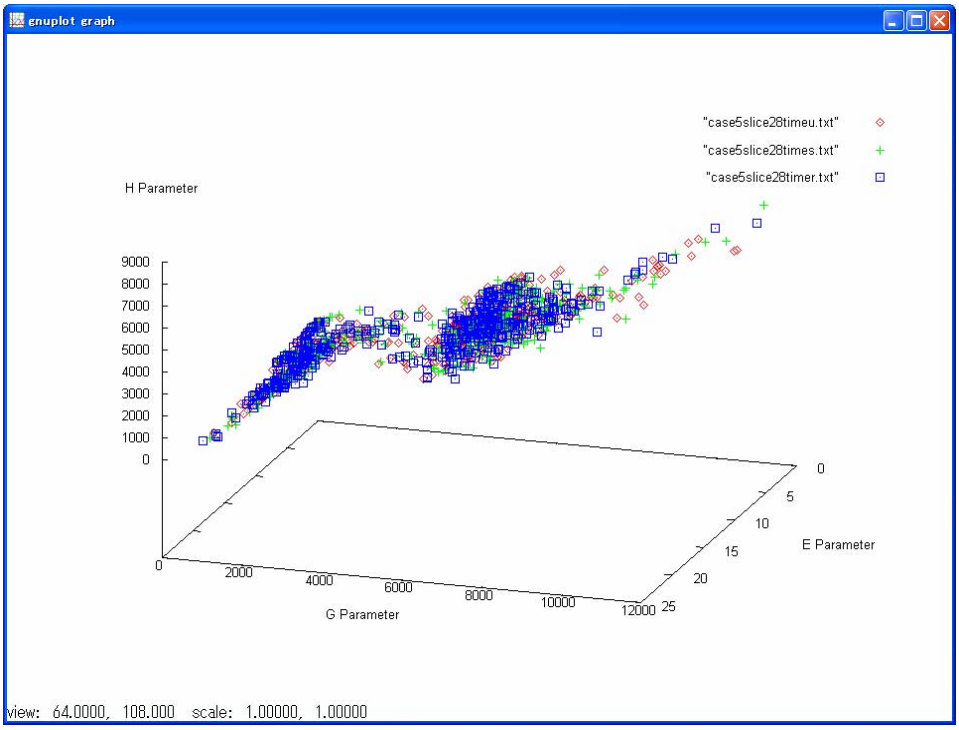

Fig. 10: Comparison of *EGH* parameter value of different time-lapse images (r, s and u), for all regions

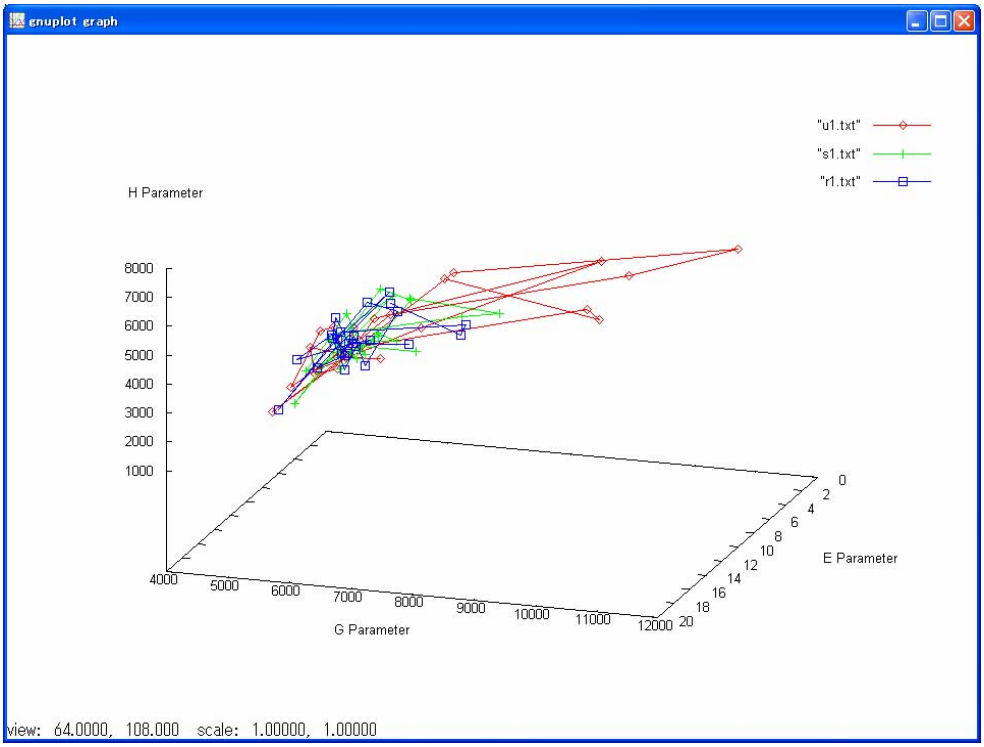

Fig. 11: Comparison of *EGH* parameter value of different time-lapse images (r, s and u) around tumor regions (totaled from 25 regions)

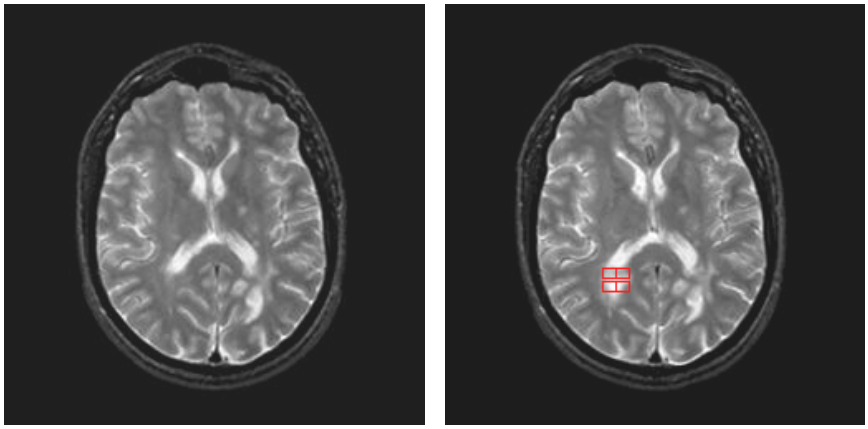

(a) (b)

Fig. 12: (a) t-interval image scan (b) PCB System detection result for abnormal regions at u-interval

5.2 Set II: Different Brain Disease Images

The proposed technique is tested on a series of T2-weighted MRI brain images from Case 1, Case 28, Case 32 and Case 33. The image is taken from patients with different chronic brain disease, as listed in Table 1. At first, each image dataset is analysed individually with experimental results shown in Fig. 13. Then, an image slice containing tumor properties is extracted from different specific tumor images to study the proposed technique for diagnosis accuracy, interpretation and robustness studies, listed in Table 2 and Fig. 14.

Table 1: Case studies from different brain diseases

Case	G_D	**Total Image Slice**	**Diagnosis**
Case 1	24.13	56	Anaplastic astrocytoma
Case 28	26.39	24	Metastatic bronchogenic carcinoma
Case 31	33.76	29	Astrocytoma
Case 32	45.14	27	Meningioma
Case 33	32.54	24	Ewing sarcoma

Table 2: Specific image slice study to compare different brain diseases and diagnosis

Case	**Image Slice**	**Clinical**
Case 1	35	Increasing right hemiparesis (weakness) and hemianopia (visual loss)
Case 28	10	History of tobacco, headaches intensified and trouble with finding words
Case 31	16	Headaches intensified and progressive symptoms
Case 32	14	History of progressive difficulties in walking, difficulties in memory and concentration, slow and hesitating speech
Case 33	11	Visual difficulties, trouble with concentration

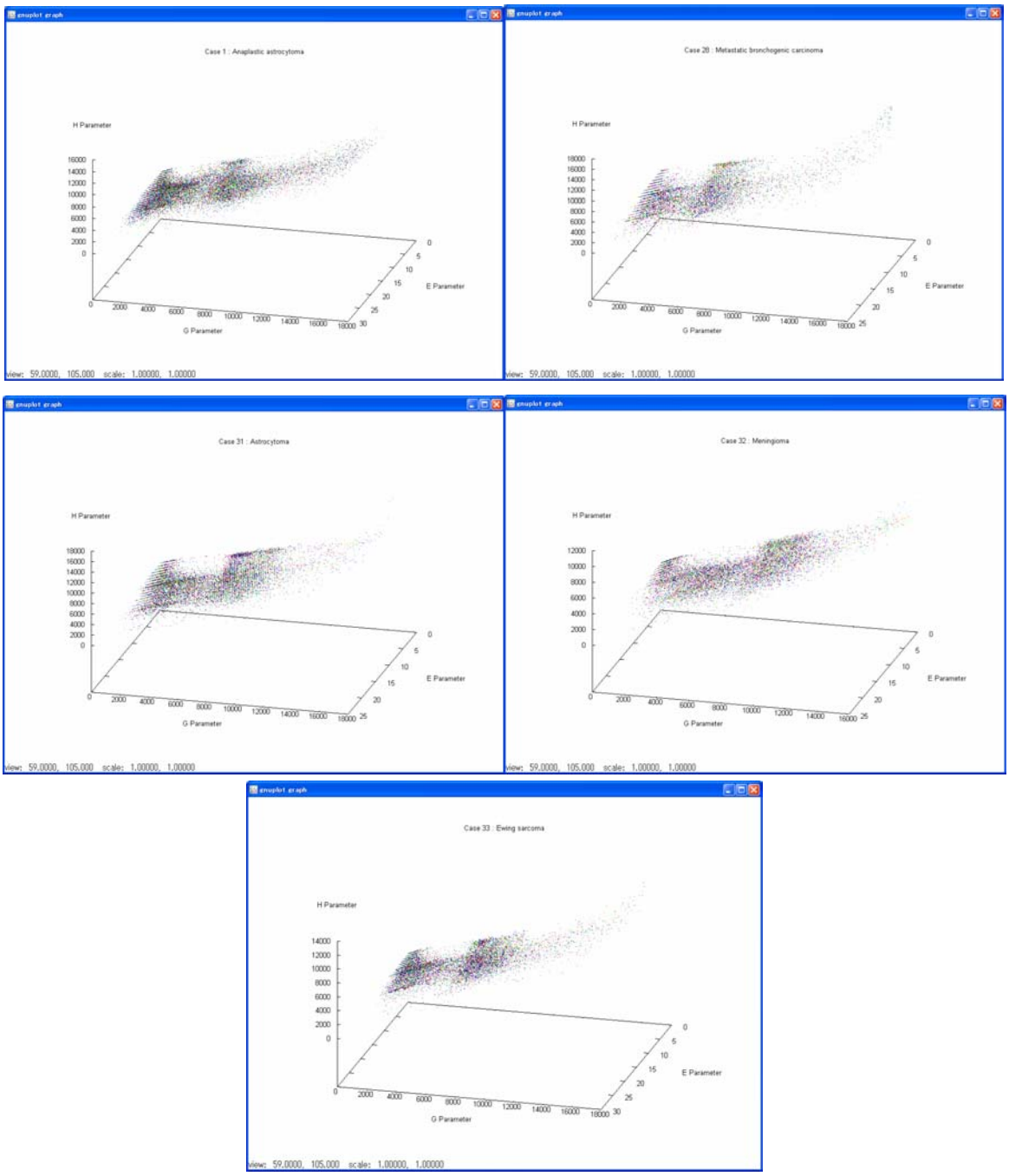

Fig. 13: Experimental result from Table 1 dataset, showing the distribution of *EGH* parameter

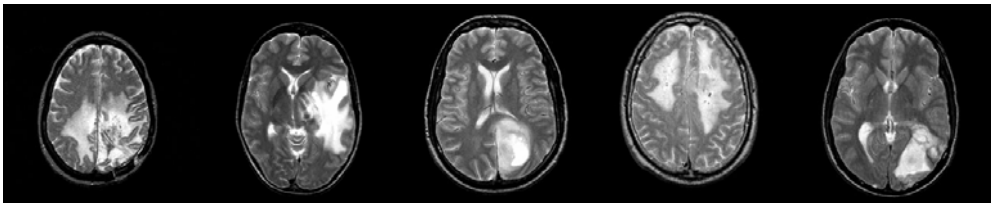

Fig. 14: Image slice selection (from Table 2), showing the tumorous regions

Fig. 13 shows that tumor regions are often associated with high *G* and *H* parameter values but low *E* parameter values. Fig. 15 shows that tumor regions are grouped at the upper-right location of the graph (marked in dotted circle), but we are not able to produce a distinct descriptor for linking and differentiating different tumor images with different brain illnesses. Fig. 16 shows the system listing of all abnormal *EGH* parameters, may suggest either a 'false alarm' in detection or a tumor region. A false alarm can occur when the input images which does not have a tumor is marked during analysis. Therefore, we further study these parameters using the PCB system to demonstrate the parameter robustness. The detection results are shown in Fig. 17. Experimental results reveal that the *EGH* parameters can accurately pinpoint the tumor regions on the image with no false alarm.

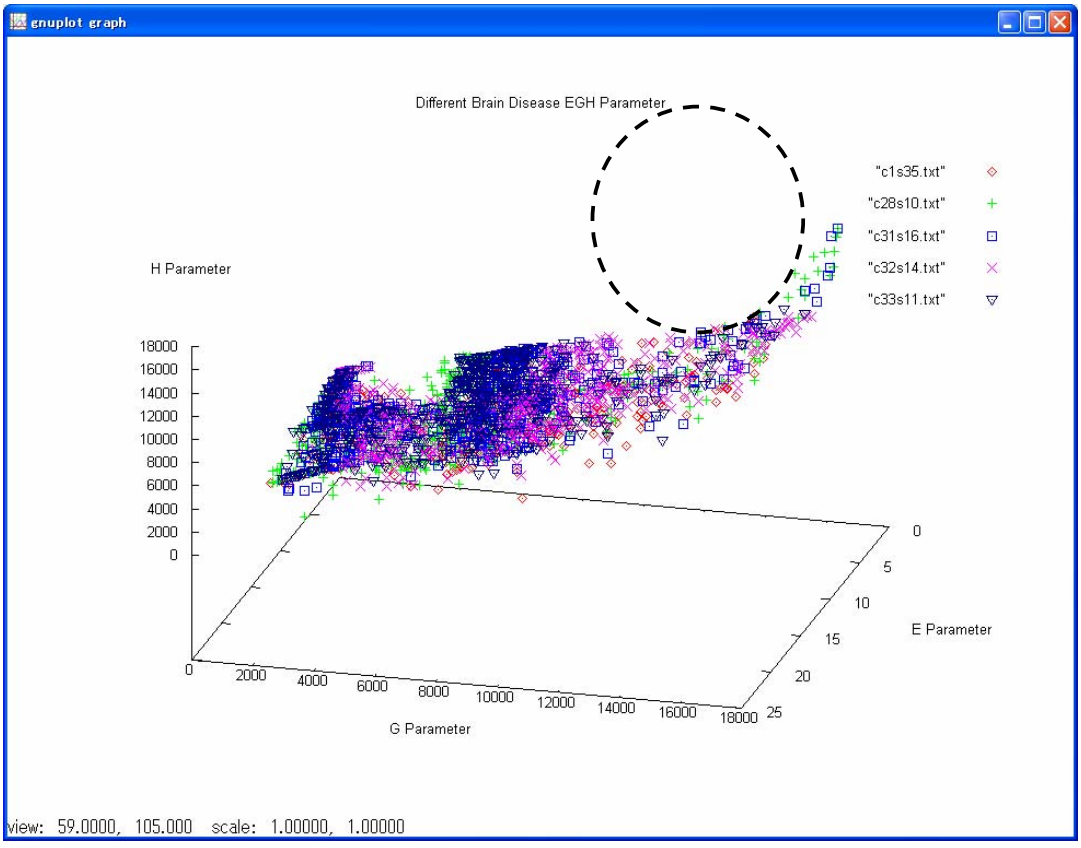

Fig. 15: Distribution of *EGH* parameters

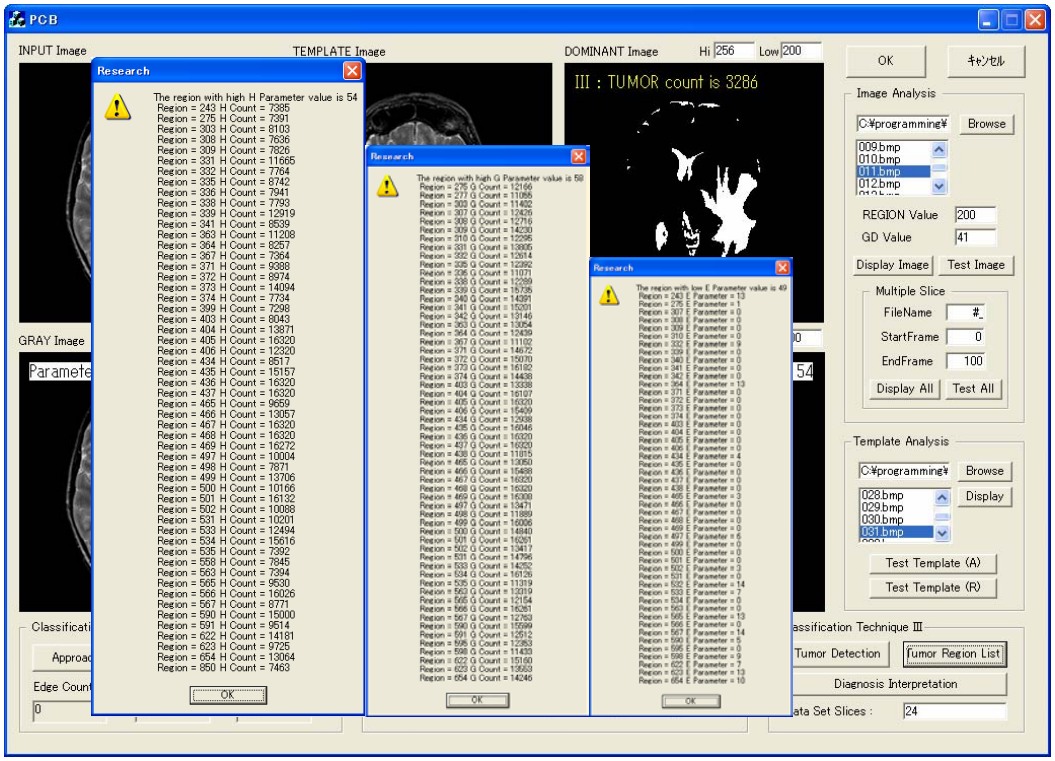

Fig. 16: Experimental image from Table II, showing the region of tumor

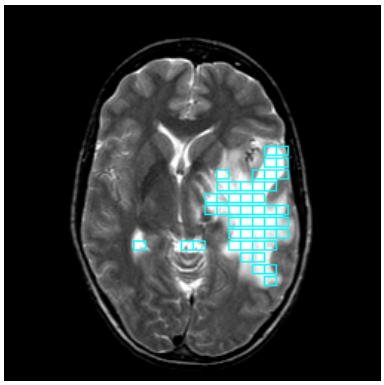

Fig. 17: Tumor regions detection result for Case 28 (Slice 10)

5.3 Set III: Different Gender and Age Brain Images for Multiple Slice Studies for Diagnosis and Interpretation

The proposed technique is tested on a series of T2-weighted MRI brain images for 9 different cases: VHD-Male, Case 1, Case 9, Case 26, Case 28, Case 31, Case 32, Case 33 and Case 36, listed in Table 3, for robustness studies. The images are taken from healthy patients as well as patients with different brain diseases**,** and the *EGH* parameter is calculated based on the image slices. We compute the values of the *EGH* parameter for the experiment image dataset using Equation (3), (4) and (6).

Table 3: Case studies from different gender patients

Case	**Gender, Age**	**Total Image Slice**	**Clinical**
VHD-M	Male, 39	34	None
Case 1	Female, 51	56	Anaplastic astrocytoma
Case 9	Female, 81	54	None
Case 26	Male, 62	24	Metastatic Adenocarcinoma
Case 28	Female, 42	24	Metastatic bronchogenic carcinoma
Case 31	Male, 35	29	Astrocytoma
Case 32	Male, 75	27	Meningioma
Case 33	Male, 22	24	Ewing sarcoma
Case 36	Female, 76	43	None

Fig. 18 shows the comparison between Case 1 with Case 9 *EGH* parameters obtained from all image slices (both female). Initial studies show that when tumor occurs in the image slice, the gray matter is occupied by a large 'white tumor spot', whereby the *E* parameter count is reduced, and the *G* and *H* parameter count are increased. According to the diagnostic information, Case 1 consists of images taken from a patient suffering from Anaplastic Astrocytoma. Using *EGH* parameter and our estimation model, we detect strong representation of tumor occurrence from slice 24 to slice 42 (totaled 19 slices) which detects the abnormal slices double-marked using a square [□] point on top of the diamond [◊] point, comparing Case 1 (represented by diamond [◊] points) and Case 9 (represented by plus [+] points), thus showing the accuracy of our proposed *EGH* parameter method. We run Case 1 image dataset on the PCB system and the detection result is shown in Fig. 19. The result reveals the accuracy of using *EGH* parameter for detecting tumorous images among the entire image dataset.

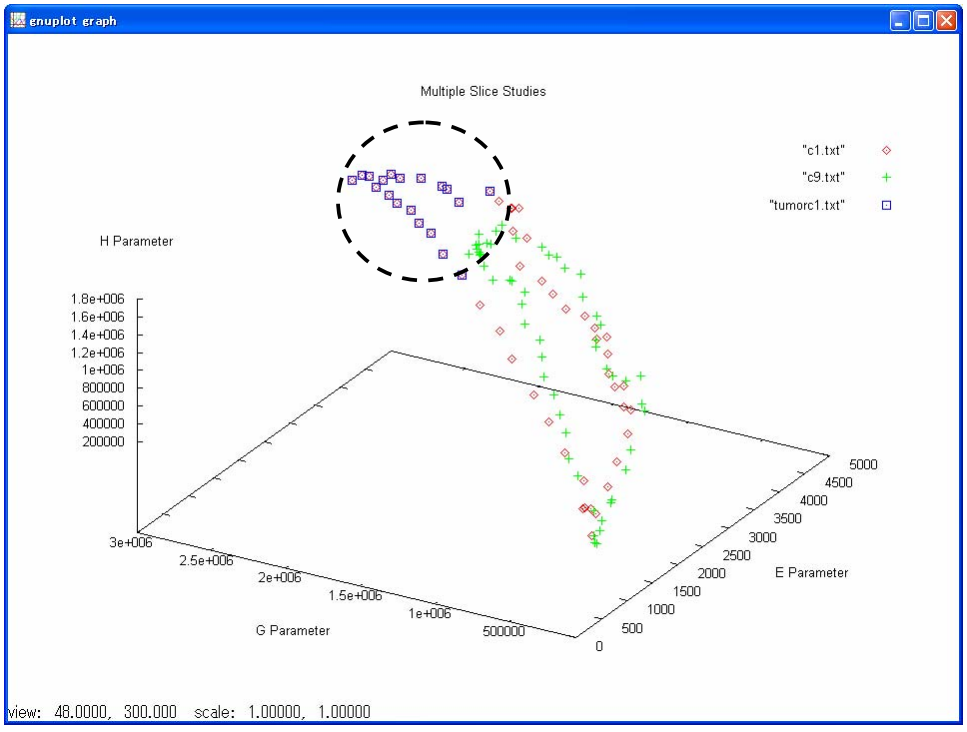

Fig. 18: Experiment image from Table 2, showing the region of tumor

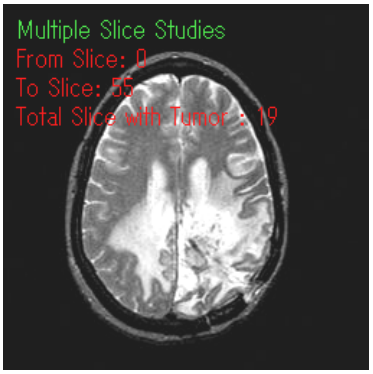

Fig. 19: Tumor image detection result on multiple image slice analysis for Case 1

In Fig. 20, the *EGH* parameter value shows a high deviation computed (left side) which clearly indicates an abnormality in these input images, indicating a possible tumor occurrence in such slices. Also, the analysis results (Set III consist of four female and five male cases) show no specific trending of *EGH* parameter distribution in male and female T2-weighted MRI brain images in our study, but the total image slices and the MRI imaging machine (low/mid/high field MRI) for the object of study are important issues.

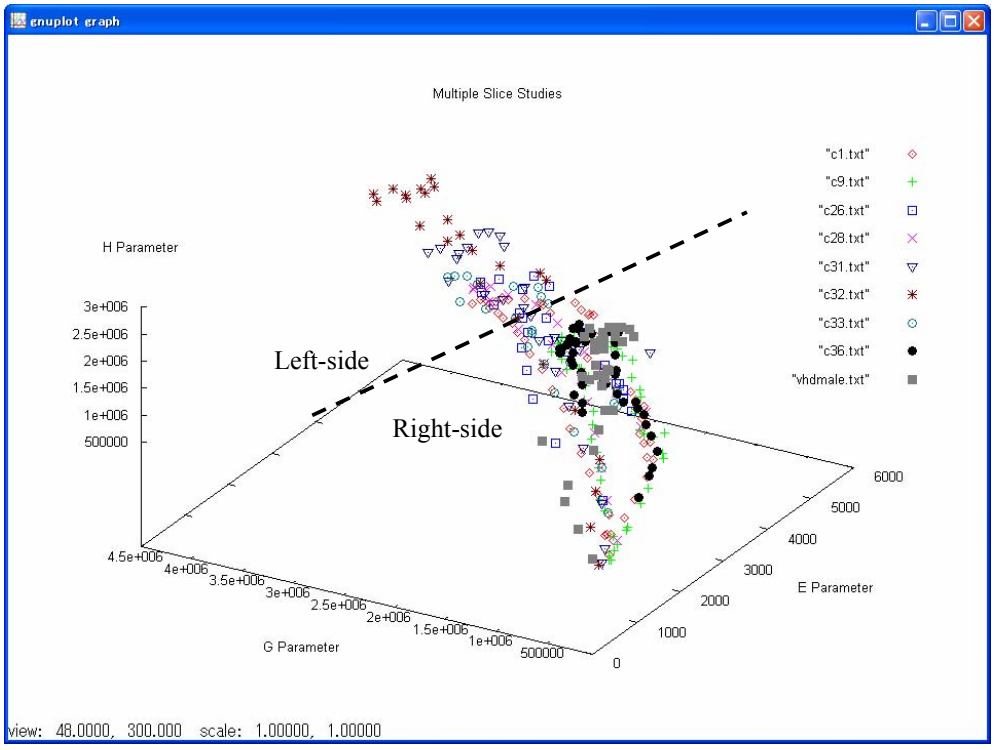

Fig. 20: Table 3 experiment dataset, showing the *EGH* parameter change over the image slice

6.0 CONCLUSIONS

In this paper, we proposed a simple multiparameter method to classify T2-weighted MRI brain images. The two techniques proposed here are experimented on three different sets of image datasets. In the first experiment (Set I), the value of the *EGH* parameter is used to define the region condition, either normal or tumor, with images obtained at different time intervals. In the second experiment (Set II), we found that the *EGH* parameter value is able to classify T2-weighted MRI brain images accurately using region-based hierarchical representation, defining regions of tumor occurrences, but are unable to produce a distinct descriptor for linking and differentiating different tumor images with different brain illness. In the third experiment (Set III), we showed that the *EGH* parameter value is able to detect tumorous input images effectively. We are able to interpret image slices "condition" using an estimation model even though we found no specific trends on the *EGH* parameter distribution in male and female images. Overall, this paper is able to identify tumor images under different circumstances and conditions. We have developed a system called '**PCB**: **P**redictive **C**ognitive System for **B**rain Images' and we are incorporating the technique proposed here for classifying images into tumor and non-tumor images. To further test the performance of our algorithms, we compare experimental results of previous proposed tumor detection method with the proposed method here, shown in Table 4. The proposed technique incurred an overall error smaller in comparison with our previous proposed method [15]. In particular, the proposed method allowed decrements of false alarm and missed alarm, which demonstrates the effectiveness of our proposed technique. However, even though in all of our experiments we have obtained a good stability, we think that a further reduction in error is necessary for the software to have commercial value and a significant competitive edge.

Table 4: Performance of the proposed multiparameter method (in *SOI*)

APPROACH	IMAGE	Previous [15]		Previous [2]		Multiparameter	
	SLICE	False Alarm	Missed Alarm	False Alarm	Missed Alarm	False Alarm	Missed Alarm
Case 1	**56**	0%	24%	5%	0%	0%	0%
Case 9	**54**	11%	-	11%	-	0%	-
Case 26	**24**	37%	50%	27%	17%	17%	11%
Case 28	**24**	5%	28%	5%	0%	0%	0%
Case 31	**29**	25%	48%	8%	5%	7%	5%
Case 32	**27**	19%	33%	15%	3%	7%	0%
Case 33	**24**	14%	25%	19%	4%	9%	4%
Case 36	**43**	10%	-	23%	-	0%	-
Overall		15%	35%	17%	40%	5%	3%

*Multiparameter and previous [2] "false alarm" and "missed alarm" is compensated by visual confirmation of images using regions (r,c)

** Case 26 – high false alarm and missed alarm is due to the cavity and low signal on T2-weighted image at the frontal lesion

Overall the proposed method shows considerable improvement over previously proposed technique. We are now in the process of studying other methods to reduce the errors produced here by introducing wavelet transformation of unsupervised region on volumetric T2-weighted MRI images. We expect that the PCB system will become a valuable tool for the study of T2-weighted MRI brain images. All our future efforts will focus on introducing other medical images, e.g. PET/CT or PET, into the PCB system via a user-friendly and practical system usable in clinics for medical specialists and medical students.

7.0 ACKNOWLEDGEMENT

The authors would like to thank all reviewers of this paper. This work is supported in part by grant from VISOR Project, a Special Coordination Funds from the Ministry of Education, Culture, Sports, Science and Technology of the Japanese Government, and The Keio Leading-edge Laboratory of Science and Technology.

REFERENCE

[1] P. Y. Lau and S. Ozawa, "Image Classification for Different Imaging Modalities in Image-Guided Medical Diagnosis Model", in *Proceeding of IEEE EMBS Asian-Pacific Conference on Biomedical Engineering*, Keihanna, Japan, 20-22 Oct. 2003, IEEE Catalog Number: 03EX711C.

[2] P. Y. Lau and S. Ozawa, "A Region- and Image-Based Predictive Classification System for Brain Tumor Detection", in *Proceeding of Symposium on Biomedical Engineering 2004*, Hokkaido, Japan, 29-30 Sept. 2004, pp. 72-102.

[3] P. Y. Lau and S. Ozawa, "Modality-based Image Registration Using Multiple Classifiers in Image-Guided Medical Diagnosis Model", in *Proceeding of Symposium on Biomedical Engineering 2003*, Hokkaido, Japan, 5-6 Sept. 2003, pp. 140-169.

[4] P. Y. Lau and S. Ozawa, "An Economic Approach to Image-Guided Medical Diagnosis Model", in *Proceeding of World Congress on Medical Physics and Biomedical Engineering*, Sydney, 24-29 Aug. 2003, Vol. 4.

[5] J. W. Bailet, E. Abemayor, B. A Jabour, R. A. Hawkins, C. K. Hoh and P. H. Ward, "Positron Emission Tomography: A New Precise Modality for Detection of Primary Head and Neck Tumors and Assessment of Cervical Adenopathy". *Laryngoscope*, Vol. 102, 1992, pp. 281-288.

[6] D. H. Miller, R. I. Grossman, S. C. Reingold and H. F. McFarland, "The Role of Magnetic Resonance Techniques in Understanding and Managing Multiple Sclerosis". *Brain*, Vol. 12, 1998, pp. 3-24.

[7] M. D. Liem, D. J. Gzesh and A. E. Flanders, "MRI and Angiographic Diagnosis of Lupus Cerebral Vasculitis". *Neuroradiology*, Vol. 38, 1996, pp. 134-136.

[8] A. Vailaya, M. A. T. Figueiredo, A. K. Jain and H. J. Zhang, "Image Classification for Content-Based Indexing". *IEEE Transactions on Image Processing*, Vol. 10 No. 1, 2001, pp. 117-130.

[9] S. Abbasi and F. Mokhtarian, "Affine-Similar Shape Retrieval: Application to Multiview 3-D Object Recognition". *IEEE Transactions on Image Processing*, Vol. 10 No. 1, 2001, pp. 131-139.

[10] Y. Deng, B. S. Manjunath, C. Kenney, M. S. Moore and H. Shin, "An Efficient Color Representation for Image Retrieval". *IEEE Transactions on Image Processing*, Vol. 10 No. 1, 2001, pp. 140-147.

[11] I. Epifanio and G. Ayala, "A Random Set View of Texture Classification". *IEEE Transactions on Image Processing*, Vol. 11 No. 8, 2002, pp. 859-867.

[12] M. Hinz, R. Pohle, H. Shin and K. D. Tonnies, "Region-Based Interactive 3D Image Analysis of Structures in Medical Data by Hybrid Rendering", in *Proceedings of SPIE (Visualization, Image-Guided Procedures, and Display),* San Diego, USA, 23-28 February 2002, Vol. 4681, pp. 388-395.

[13] A. V. Thamburaj, "Neurology & Systemic Malignancy", Apollo Hospitals, Chennai, India http://www.thamburaj.com/cns_systemic_malignancy.htm

[14] H. A. Vrooman, P. J. M. Rietveld and P. van Dijk, "Semi-Automated Detection of White Matter Lesions by Contrast Optimization and 3D Region Growing in MR Data of the Brain", in *RSNA 2001: 87th Scientific Assembly and Annual Meeting of the Radiological Society of North America*, Chicago, IL, 25-30 Nov. 2001, Vol. 221, p. 460.

[15] P. Y. Lau and S. Ozawa, "PCB : A Predictive System for Classifying multimodal Brain Tumor Images in an Image-Guided Medical Diagnosis Model", in *Proceeding of the 12th International Conference on Intelligent System for Molecular Biology*, Glasgow, UK, 31 July – 4 Aug. 2004.

[16] K. Krishnan and M. S. Atkins, "Segmentation of Multiple Sclerosis Lesions in MRI - An Image Analysis Approach", in *Proceeding of the SPIE in Medical Imaging 1998*, San Diego, CA, 21-27 February, 1998, Vol. 3338, pp. 1106-1116.

[17] R. Gupta and P. Undrill, "The Use of Texture Analysis to Delineate Suspicious Masses in Mammography". *Physics in Medicine and Biology*, Vol. 40, 1995, pp. 835-855.

[18] C. R. G. Guttmann, F. A. Jolesz, R. Kikinis, R. J. Killiany, M. B. Moss, T. Sandor and M. S. Albert, "White Matter Changes with Normal Aging". *Neurology*, Vol. 50, 1998, pp. 972-978.

[19] L. F. Donnelly, MD. *Pocket Radiologist Pediatrics 100 Top Diagnoses*. W. B. Saunders Company, 2002.

BIOGRAPHY

Phooi Yee Lau received her B.Sc. from University of Teknology Malaysia in 1996, and her M. Sc. from University of Malaya, in 2002. From 1996 to 2001, she worked for Matsushita as a systems engineer. She is currently working towards her Ph.D. degree at Keio University. Her current research interests are in medical image processing and intelligent systems. She is currently a student member of the IEICE, IEEE, and ISCB.

Shinji Ozawa received the B.E., M.E. and Ph.D. degrees all in Electric Engineering from Keio University, Japan in 1967, 1969 and 1972, respectively. He has been employed as a Research Associate, Assistant Professor and Associate Professor from 1970 in the Department of Electric Engineering of Keio University. He is currently a Professor in the Department of Information and Computer Science at Keio University. In 1984, he was a Visiting Professor at University of Maryland, USA. His research interests include digital communication and signal processing on image and voice. He is a member of IEICE, IPSJ, IEEE, and a fellow of IAPR.